

D. Wüster

H. Vernickel, J. Bohdanský, H.J. Kutsch,
W. Ottenberger, J. Roth, R. Scherzer, F. Steinberger, E. Trčka

**GAS UPTAKE
BY COATED AND UNCOATED GRAPHITE
EXPOSED TO AIR**

H. Vernickel, J. Bohdanský, H.J. Kutsch,
W. Ottenberger, J. Roth, R. Scherzer, F. Steinberger, E. Trčka

IPP 1/239

February 1987



MAX-PLANCK-INSTITUT FÜR PLASMAPHYSIK

8046 GARCHING BEI MÜNCHEN

MAX-PLANCK-INSTITUT FÜR PLASMAPHYSIK
GARCHING BEI MÜNCHEN

GAS UPTAKE
BY COATED AND UNCOATED GRAPHITE
EXPOSED TO AIR

H. Vernickel, J. Bohdanský, H.J. Kutsch,
W. Ottenberger, J. Roth, R. Scherzer, F. Steinberger, E. Trcka

IPP 1/239

February 1987

Die nachstehende Arbeit wurde im Rahmen des Vertrages zwischen dem Max-Planck-Institut für Plasmaphysik und der Europäischen Atomgemeinschaft über die Zusammenarbeit auf dem Gebiete der Plasmaphysik durchgeführt.

GAS UPTAKE BY COATED AND UNCOATED GRAPHITE EXPOSED TO AIR

H. Vernickel, J. Bohdansky, H.J. Kutsch,
W. Ottenberger, J. Roth, R. Scherzer, F. Steinberger, E. Trcka

Abstract

When tokamaks are vented, as is inevitable for repair and modification work, graphite components should adsorb as little gas as possible. This reduces the risk of uncontrolled gas desorption in tokamak operation. The purpose of this investigation is to determine whether various types of graphite differ with respect to gas adsorption and whether a low-Z coating with pyrocarbon or silicon carbide might possibly significantly reduce gas uptake.

The investigation was concerned with the gas release of samples in the state in which they were delivered by various manufacturers and with the subsequent gas uptake when they were exposed to air after degassing. There were no drastic differences between the graphites investigated. Pyrocarbon coating does not reduce the short-time gas adsorption within 1 - 2 days, slows down further gas adsorption by a factor of up to 10 in one case, and not at all in another case. The cause of these big differences has not been clarified. Coating with SiC has just a small influence on gas adsorption. Mass spectrometric investigation of the desorbed gas shows appreciable differences in gas composition and desorption temperature with about equal weight loss. The causes of these differences are not known either.

1. Introduction

Graphite as a refractory low-Z material is being increasingly used for high-heat-flux in-vessel components and for lining the first wall of tokamaks and stellarators. Besides the price, the following criteria are important for selecting the best type of graphite. The weighting of the individual points is governed by the specific application. The type of graphite preferred for a limiter may possibly be different from that selected for a covering tile situated far from the plasma, since the tile is not subjected to a particularly high thermal load. The selection criteria are as follows:

1. good heat conduction and high heat capacity;
2. low sputtering erosion;
3. high mechanical strength;
4. low erosion with (short-time) thermal overload;
5. resistance to mechanical damage due to thermal shock;
6. sufficient purity (see Annex 2);
7. low gas content and low gas uptake when exposed to air insofar as the gases are not released during the pump-off process or at least at the baking temperature (owing to the risk of release in the event of uncontrolled temperature rise during operation);
8. small influence on density control and isotope composition of the plasma;
9. the resistance to neutron radiation, which is important for reactors, does not play any role in present devices; for ASDEX Upgrade the collection of tritium is of no consequence either.

The purpose of the present investigation was to obtain some data on point 7., since very little information is available in the literature. In particular, it was to be clarified whether gas adsorption can be significantly reduced by means of vacuum-tight coating. The conditions to be met by the coating were: good adhesion when subjected to thermal cycling, electrical conductivity (no special requirements, but the layer should not be an insulator) and finally the layer should not contain any elements with atomic numbers higher than 14. (This ruled out TiC, which is otherwise often used.)

2. Selection of Samples

The present selection of samples is mainly based on coating systems which were short-listed on the basis of proposals made by firms for ASDEX Upgrade, the uncoated graphites being given for comparison.

The samples were disc-shaped according to Fig. 1a (sample A) and cylindrical according to Fig. 1b (sample B). It was specified that the samples be dedusted in an ultrasonic bath after mechanical production, be degassed in vacuum at $T \gtrsim 1500^\circ\text{C}$, and finally (or after coating) be packed in foils impermeable to water vapor, e.g. Hostaphan.

Coatings: in these test pyrocarbon (designated as PyC in the following) and SiC layers produced by the CVD method were investigated. The thickness of the PyC layers is between 20 and 30 μm (according to the manufacturer's specifications) that of the SiC layer 30 μm (EK96) or 100 μm (FE98). The structures of the layers in the scanning microscope were similar. Figure 2 shows an example of a PyC layer and an example of an SiC layer.

The samples have bores for accommodating fastening screws (Fig. 1a) or for attaching thermocouples (Fig. 1b). These locations are certainly only poorly coated or not at all. This can hardly be avoided in actual components either.

The samples 1346 PT and 5890 PT used in the following are designated for short as 1346 and 5890.

3. Degassing Measurements on Samples in the Condition as Supplied

Two different measurements were made, viz. the weight loss and gas volume desorbed. The degassing rate was measured with the Duran glass apparatus according to Fig. 3. The sample was pumped with the calibrated conductance of $L = 0.45 \text{ l/s}$ (at room temperature). The degassing rate is then $(p_2 - p_1)L$. The part of the apparatus indicated in Fig. 3 can be heated to 150°C . The measurements were made

- a) for 24 h at room temperature
- b) then for 24 h at 150°C , and
- c) after recooling to room temperature. Two samples each of type B) were used for these measurements. Their total mass is 2.9 g. The quantity of gas desorbed is determined by integrating the degassing rates over time.

Typical results are shown in Fig. 4. The furnace was switched on at time $t=0$; the maximum degassing rate occurred shortly before $T = 150^{\circ}C$ was reached. The time integrals of all measurements minus the background are presented in columns 1 and 2 of Table I. Column 3 is the sum of columns 1 and 2, with respect to a sample mass of 1 g, and with the assumption that the molecular weight $M = 18$.

The weight loss incurred by samples A) when first baked to $750^{\circ}C$ was measured with the apparatus described in detail in Section 5. The data are listed in column 4 of Table I. Column 5 then gives these data again with respect to 1 g.

The assumption that the molecular weight is $M = 18$ is correct when the desorbed gas is water, but it is also a useful approximation for a mixture of H_2 and CO .

The relatively good agreement of the data in columns 3 and 5 of Table I is a clear indication that the gas desorption scales as the mass and not as the surface area: whereas the mass ratio of the samples is between 6 and 8, the surface ratio is close to 2. Scaling as the surface area would thus yield a much smaller gas desorption for the samples baked at the higher temperature. The same applies to the coated samples.

From one sample (EK96) it was found that for this graphite the weight loss after 24 h at $150^{\circ}C$ was only half the total weight loss after degassing at $750^{\circ}C$.

4. Degassing Rates after Baking at $150^{\circ}C$

The degassing rates for all samples after 25-hour degassing at $150^{\circ}C$ followed by cooling to room temperature were within the normal fluctuations of the background of the apparatus, viz. $5 \cdot 10^{-9} Pa m^3/s$ which corresponds to approx. $2 \cdot 10^{-6} Pa m^3/kg$ s, if scaling as the mass is also used here. This value, however, is only the upper limit.

A supplementary measurement with a 15 g heavy disc made of EK98 yielded the same final value for the degassing rate, so that for this graphite one can give an upper limit of $3 \cdot 10^{-7} Pa m^3/kg$ s. The pretreatment was different from that for the other samples: the disc was not made of pre-degassed graphite, but was pre-degassed at $900^{\circ}C$ in a vacuum of approx. $5 \cdot 10^{-4} Pa$ and then stored for 4 months in laboratory air. In contrast, a disc that was not pre-degassed at all yielded a marginally measurable final value of $2 \cdot 10^{-6} Pa m^3/s$ or $1.3 \cdot 10^{-6} Pa m^3/kg$ s after 24 h at $150^{\circ}C$ followed by cooling. The total quantity of desorbed gas was about $13 Pa m^3/kg$ in both cases.

5. Gas Uptake during Exposure to Air

Samples of type A (Fig. 1a) were degassed at 750°C in the sputtering apparatus described in [1] and the change in weight was determined with the installed vacuum microbalance (Mettler ME21) (see section 3). The samples were heated by bombarding the rear side with electrons. The vacuum during the baking process is approx. 10^{-5} Pa . The sensitivity of the balance is $0.3\ \mu\text{g}$. Zero drift during the measurement limits the accuracy to $\pm 1\ \mu\text{g}$. After being degassed, the samples were exposed to air and the increase of weight was measured as a function of time, partly with a normal micro balance in air (Mettler ME22). This balance is reproducible to $\pm 2\ \mu\text{g}$.

After being degassed in vacuum, all samples first show a fast weight increase within the first 30 min which then becomes much slower. After about 2 days the further slow growth in weight can be taken as roughly linear in time within a considerable range of fluctuation of the experimental data. There is still no saturation even after 50 days.

Figures 5 – 7 show the original experimental data for three examples. The strong fluctuations according to Figs. 5 and 6 are typical of the measurements on uncoated samples; we have no explanation for this. With the exception of FE219/PyC, the coated samples show much smaller fluctuations. The results are listed in Tables II and III. Table II contains original experimental data and the weight of the samples. Test series 1 and 2 were measured on various samples of the same batch. The procedure was as follows: the sample was degassed in vacuum at 750°C and then weighed in vacuum. The sample was withdrawn and after 30 min was again inserted in the vacuum and weighed. The difference is given in column A. It was then degassed again and weighed; the difference is given in column B; after being withdrawn again, it was weighed after 30 min on the normal balance and reweighed at certain intervals (Figs. 6 – 8). The increase in weight after 50 days including that in column A is given in column C. Then reintroduction to vacuum, weighing, degassing, weighing. The difference is recorded in column D. If the measured effect is pure adsorption and desorption, columns C and D should show the same value. With few exceptions, however, D is larger than C. This would be expected if, for example, adsorbed H_2O is desorbed as $\text{H}_2 + \text{CO}$ after chemical reaction. If the total weight increase is H_2O and is only desorbed as $\text{H}_2 + \text{CO}$, one would get $\text{D}/\text{C}=1.66$. The measured values are almost all smaller. As discussed below, distinct desorption of H_2O is only observed by mass spectroscopy in the two PyC-coated samples 5890 and 1346 (not in the other two PyC-coated samples). In these two samples D/C is in fact close to 1. With EK98, on the other hand, it is predominantly desorption of H_2 and CO that is found, although D/C is likewise close to 1.

As can be seen in Figs. 5 -7, in the period between 2 and 50 days the weight increases linearly with time - within an appreciable range of fluctuation. Since, moreover, the weight increase is proportional to the mass (as shown above), the data can be stated in the form

$$\frac{\Delta m}{m} = a + bt \quad \text{for } 2d \lesssim t \lesssim 50d. \quad (1)$$

In Table III all the gas adsorption measurements are presented by stating the constants a and b .

In addition, Table III contains some experimental data measured after even longer times and the values calculated with eq. (1) for these times. In the samples with slow gas adsorption there is still no sign of saturation even after 125 days; in contrast, the samples with fast gas adsorption show saturation. It could be speculated that saturation occurs at $\Delta m/m$ of about 10^{-4} . For shorter times the situation is as follows: the gas adsorption within 1 - 2 days, which is characterized by the constant a in Table III, is around $(30 \pm 15) \mu g/g$ for all samples investigated, irrespective of the coating. For longer times the coating generally slows down the gas adsorption. The reason for the different behaviour of similar coating systems from different suppliers is unclear.

Similar investigations at the Sandia Laboratories [2] yielded, firstly, with one exception, roughly the same gas adsorption by all types of graphite measured within two days; secondly, in comparable samples a factor of approx. 2 larger gas adsorption, which, however, can be regarded as agreement since the measurements are quite different, viz. in [2], measurement of the desorbed gas volume and, in our case, the increase in weight.

6. Mass-spectroscopic Determination of the Desorbed Gases

Mass spectra were recorded during degassing according to 3.1. This was done with a quadrupole MS (QM511) whose ion source was aligned in the direct line of sight of the sample.

The measurement was concerned with the intensity of the mass signal as a function of time, i.e. the sample temperature, as well as with mass scans. The scan time for a mass spectrum was small compared with the heating time.

The most important components found are hydrogen (H_2), water vapor (H_2O) and carbon monoxide (CO). While water shows a characteristic desorption maximum between

300°C and 330°C, this was not found for H_2 and CO . Figure 8 shows a desorption spectrum for water. A graphite sample (FE159i, graphite limiter of ASDEX) was degassed, being heated first to 1000°C and then exposed to air for 67 hours. The 0.739 g heavy sample gained 40 μ g in weight.

Other types of graphite, such as EK96, did not show this water desorption. Figure 9 shows desorption spectra of a graphite sample of type EK96. Water shows merely a hint of a desorption maximum at 300°C, while hydrogen and carbon monoxide still exhibit a high degassing rate at 750°C. From measurements made at Sandia Laboratories [3] we know that CO and H_2 show a drastic rise in the degassing rate at temperatures above 1000°C. This may explain the large scatter in the weight loss measurements because there might be smaller or larger amounts of these gases in the graphite, depending on the pre-treatment.

The weight loss in air is by no means solely due to the higher degassing rate of water. Figure 10 shows the desorption spectrum of various coated and uncoated samples. After being baked at 1000°C, all samples were exposed to air for 20 h. They were then raised to a temperature of 750°C at a heating rate of 2°C/s and the desorption spectrum was measured. The weight loss Δg incurred during baking is also shown in the figure. Independently of whether water desorption occurs or not, the weight loss is similar for the different samples stated. This finding is difficult to understand and may be connected with the fact that adsorbed H_2O is dissociated in some samples and not in others. With samples of 5890PT belonging to different batches, it was predominantly desorption of H_2O that was found one time, and of H_2 and CO another time. The reasons for these differences are not known either.

7. Resistance of the Coating to Thermal Cycling

These measurements were made with a light beam apparatus. This consists in focussing the radiation of a high-pressure xenon lamp through a window onto the sample in vacuum by means of an ellipsoid mirror. The intensity distribution in the "focus" can be approximated by a Gaussian distribution. We achieved a maximum load of 0.6 kW/cm² and a mean load of 0.48 kW/cm² with a sample diameter of 1 cm (further data in [4]). The beam was pulsed by means of a mechanical, water-cooled and automatically controlled aperture.

All coated samples were subjected to 250 load cycles with this apparatus. A cycle consists in: heating the sample from 200°C to 900°C in 7s, and cooling it to 200°C in

4.8 min. Two samples (EK96/PyC and FP98/SiC) were heated 1250 times. The SEM photos showed no failure of the coating, i.e. no flaking or the like. EK96/SiC did show the odd crack, but similar cracks were already found in one sample before irradiation. Occasional rosette-shaped bursting of the humps was observed in the PyC layers on FP219 and EK96 (see Fig. 11).

These structures were already present after 250 cycles; their frequency did not significantly increase between 250 and 1250 cycles.

8. Conclusion

With respect to gas uptake, the samples coated with SiC are not better than uncoated ones as regards short-time behaviour, and not much better as regards long-time behaviour. The short-time behaviour of PyC-coated graphites is not better either than that of uncoated graphites; but with one exception, namely FP219/PyC, the long-time behaviour is considerably better: EK96 PyC, 1346 PyC and 5890 PyC in that order. The temperature cycling was positive on the whole; details are discussed above.

The uncoated graphites are almost identical to one another in their short-time behaviour; only 1346 PT and 5890 PT show slightly poorer performance. The differences in long-time behaviour are smaller, there being a factor of about 1.5 between the best and the poorest of the samples investigated. The order found from all gas uptake/degassing measurements is roughly EK96, FP98, FP219, EK98, these being almost equal, and 5890, 1346 with some difference, particularly owing to the large 30-min value and the high degassing of the samples in the state delivered.

Comparison between EK96 and EK96/PyC finally shows: the initial value of the coated graphite is somewhat better, and the long-time value is a factor of about 3 better.

It should be pointed out that all measurements discussed here were made on small samples weighing between 0.5 and 3 g (and in one case 15 g). It is presumed that particularly the time evolution of the gas adsorption and desorption is distinctly slower in the case of large tiles.

Annex 1: Further Remarks on the Choice of Graphite

In addition to the selection criteria stated in the introduction, the following should be noted.

The density ρ of the graphites discussed in general is between 1.65 and 1.85 g/cm³, and the specific heat c is independent of the type. The heat capacity ρc with respect to the volume thus varies by less than 10 %, which has no bearing on the selection.

Erosion due to sputtering, both chemical and physical, is independent of the type [5]. No significant differences in gas adsorption and desorption are known either [6]. Criteria 2 and 8 of the introduction thus afford no help in reaching a decision.

The thermal conduction, mechanical strength, thermal expansion and Young's modulus, i.e. the parameters which govern criteria 4 and 5, are strongly temperature-dependent. The response is in general the same for all types of graphite, but the quantitative dependence is type-dependent. The specification of characteristics, such as the thermal shock parameter $\frac{\sigma\lambda(1-\nu)}{\alpha E}$ or $\frac{\sigma\sqrt{\lambda\rho c}}{\alpha E}$, is therefore only relevant if these quantities are known in the entire temperature range covered. Even differences in the characteristics of 50 % at room temperature tell us nothing about which type behaves better at 1000°C or 1500°C.

Calculations of the erosion depth are not sufficiently accurate: H. Nakamura et al. [10] find in the case of electron bombardment of ATJ and IG-11 graphite with 1.1 kW/cm² for 30 s, an erosion which is about twice as large as calculated and which is also equal for both graphites and not lower for IG-11, as expected.

Correlations between the selection criteria of the introduction and easily accessible list data are not known or are not definite. For example, the gas adsorption measured here does not correlate with the density (i.e. the total porosity), nor with the gas permeability. In some graphites investigated in JET [7] the erosion due to excessive thermal load correlates with the density. In contrast, the values reported by Bohdanský et al. [3] do not show this correlation. It follows from this that the requirements of fine-grain quality, low porosity or low permeability to gas cannot be justified.

The situation is similar for the isotropy: it facilitates thermomechanical calculations, but moderate anisotropy does not appear to cause any trouble (under certain circumstances, it could be of advantage in the proper direction).

No mention has been made of the electrical conductivity. It is desirable to prevent (undefined) static charging; it should be as small as possible in order to keep the currents

induced by disruption and the associated mechanical loads small. The usual value of the specific resistance of a few $10^{-5} \Omega m$ happens to be a favourable compromise, the exact value being uncritical.

Annex 2: On the Purity Required of the Graphites

As the graphites are subjected to very high temperatures in production, it is assumed that there is subsequently no longer any surface segregation of impurities. In the stationary state the impurities are then ejected by sputtering in accordance with the relative concentration. Furthermore, we assume that the permissible quantity of impurities in the plasma is governed by the radiation loss, require that the impurities cause locally 10 % at most of the radiation loss due to the graphite, and assume that the penetration probability for graphite and impurity atoms is equal. As a measure of the radiation we use radiative cooling rates with corona equilibrium in accordance with [8]. The following table gives the ratio of the cooling rates of Si and Fe, divided by the cooling rates of graphite, at the same temperature:

T_e (keV)	0.01	0.1	1	10
Si/C	< 1	90	50	10
Fe/C	~ 1	400	850	75

It can be seen that an atomic concentration of Si in the ratio 1 : 10^3 or of Fe in the ratio 1 : 10^4 is harmless in the above-defined sense. This would correspond to an "ash content" of 2300 and 470 wt. ppm in the case of Si and Fe, respectively. We conclude that an ash content < 200 ppm is sufficient and up to 500 ppm is still admissible. Even this requirement is exaggerated if the graphite surface is contaminated with metals after a short period of operation, as is mostly the case with present tokamaks (see, for example, [9]).

Annex 3: Relative Emissivity of the Coatings

The light beam apparatus (see section 7) was used to measure the relative emissivity ϵ from the heating rate of the samples under otherwise equal conditions. The temperature was measured with a thermocouple in the bore shown in Fig. 1b. The EK96 samples were used for the measurement. The SiC-coated sample was heated fastest. If it is given an $\epsilon = 1$, one obtains

- $\epsilon = 0.92$ for EK96, uncoated
- 0.76 for EK96/PyC
- 0.84 for a reference sample of FE91

Literatur

- [1] H.L. Bay, J. Roth, J. Bohdanský, *J. of Applied Physics*, **48**, (1977) 4722.
- [2] A.E. Pontau, D.H. Morse, *J. Nucl. Mater.* **141-143** (1985), 124
- [3] J. Bohdanský, C.D. Croessmann, J. Linke et al.,
Nucl. Instr. Meth., accepted for publication.
- [4] H.-J. Kutsch, IPP-Report May 1986 (in German).
- [5] R. Yamada, K. Nakamura, K. Sone, M. Saidoh, *J. Nucl. Mater.* **95** (1980), 278
- [6] W. Moeller, private communication.
- [7] H. Brinkschulte, private communication.
- [8] D.E. Post, R.V. Jensen, C.B. Tarter, W.H. Grasberger, W.A. Lokke, *Atomic Data and Nucl. Tables* **20** (1978) 397.
- [9] R. Behrisch, J. Ehrenberg, H. Bergsaker et al, to be published in *J. Nucl. Mat.* (1987).
- [10] H. Nakamura, S. Niikura, T. Uchikawa et al, JAERI- Report No. M 86-048 (March 1986).

Table I: Gas release of the as-delivered samples

	Outgassing of samples type "a"			weight loss of samples type "b"	
	24 h at room temp. 10^{-3} Pa m ³	24 h at 150° C 10^{-3} Pa m ³	total outgassing $\mu\text{g/g}$ (1)	weight loss after 750° C μg	specific weight loss $\mu\text{g/g}$
EK96	1.5	20	55	15	34
5890	4.9	103	280	88	238
1346	17.3	90	280	103	260
FP219	1.5	21	59	8	24
FP 98	1.2	11	30	9	25
EK96/PyC	0.9	9	26	15	33
5890/PyC	2.5	39	107	26	65
1346/PyC	1.5	20	55	17	41
FP219/PyC	(no data)	11	31	7	21
EK96/SiC	1.7	11	33	27	55
FP98/SiC	6.7	16	59	18	47
no sample (background)	0.5	2	6	-	-

1) Sum of first two lines per g of sample mass, with the assumption that the molecular weight $M = 18$

Table II: Gas uptake during exposure to air

Sample	run	<div style="text-align: center;"> μg </div>				D/C	weight of sample g
		A	B	C	D		
EK96	1	2.5	2.5	29	34	1.17	0.43
	2	5.0	-	23	36	1.57	0.44
5890	1	6.0	6.0	39	52	1.33	0.37
	2	7.5	-	26	35	1.35	0.37
1346	1	6	6	44	50	1.14	0.39
	2	6.5	-	38	45	1.18	0.40
FP219	1	2.5	3	28	40	1.43	0.33
	2	6	-	24	32	1.33	0.34
FP98	1	2.5	3	29	31	1.07	0.36
	2	6.0	-	24	32	1.33	0.36
EK98	1	(3)	-	43	42	0.98	0.50
	2	5.5	-	34	36	1.06	0.41
-	-	-	-	-	-	-	-
EK96/PyC	1	2.5	2.5	8	14	1.75	0.46
5890/PyC	1	11	11	28	20	0.71	0.40
1346/PyC	1	7	8	15	15	1.00	0.41
FP219/PyC	1	2.5	2.5	33	37	1.12	0.34
	2	5.0	-	26	28	1.08	0.34
-	-	-	-	-	-	-	-
EK96/SiC	1	3.5	3.5	21	24	1.14	0.49
FP98/SiC	1	3.5	4	24	32	1.33	0.38

A: Weight gain during 30 min air exposure

B: Weight loss by degassing following A

C: Weight gain during 50 d air exposure

D: Weight loss by degassing following C

Note: $D/C = 1.66$, if $\text{H}_2\text{O} \rightarrow \text{CO} + \text{H}_2$

Table III: Gas uptake during exposure to air

Data are presented according to

$$\frac{\Delta m}{m} = a + bt \quad (2d \leq t \leq 50 \text{ d}) \quad (1)$$

Sample	50 day exposure		long term exposure		
	$a \cdot 10^6$	$b \cdot 10^6/d$	$10^6 \frac{\Delta m}{m}$ (eq. 1)	$10^6 \frac{\Delta m}{m}$ (measured)	exposure (d)
EK96	17	0.8	117	79	125
			251	195	292
5890	32	1.1			
1346	35	1.4			
FP219	24	1.0			
FP98	20	1.0			
EK98	18	1.3			
EK96/PyC	18	0.1	31	37	125
5889/PyC	43	0.4	93	85	125
1346/PyC	29	0.2	54	50	125
FP219/PyC	25	1.1	163	105	125
EK96/SiC	20	0.5	83	53	125
FP98/SiC	20	0.9	133	65	125

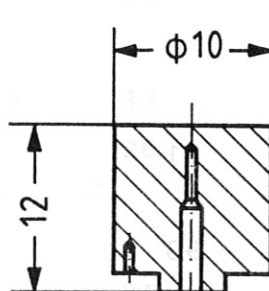
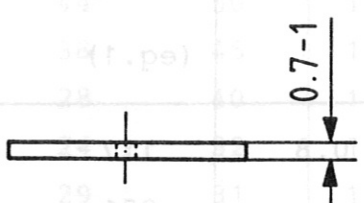
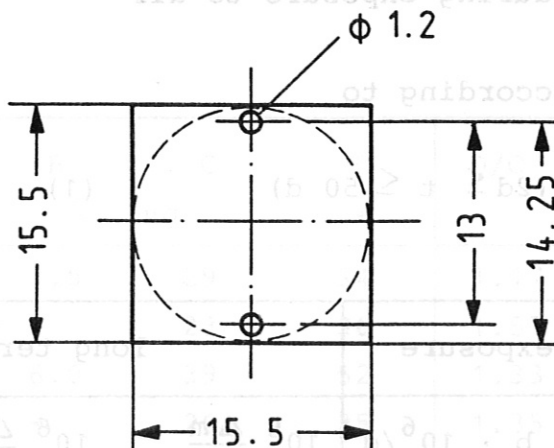
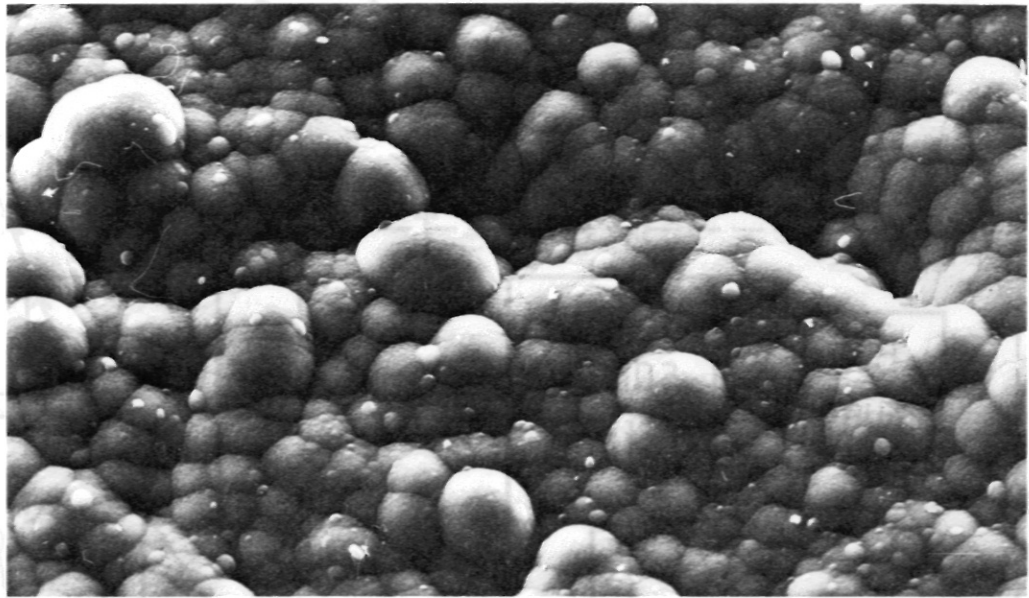
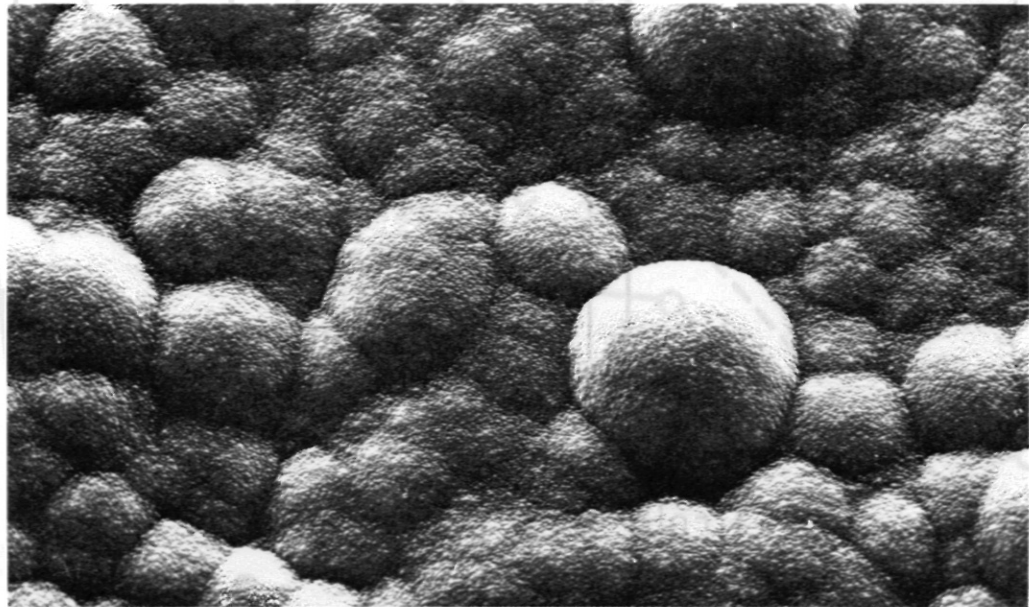


Fig. 1: Dimensions of the samples.



40 μm

a



20 μm

b

Fig. 2: Surface structure of the coatings as seen by SEM;
 a) PyC coating; b) SiC coating.

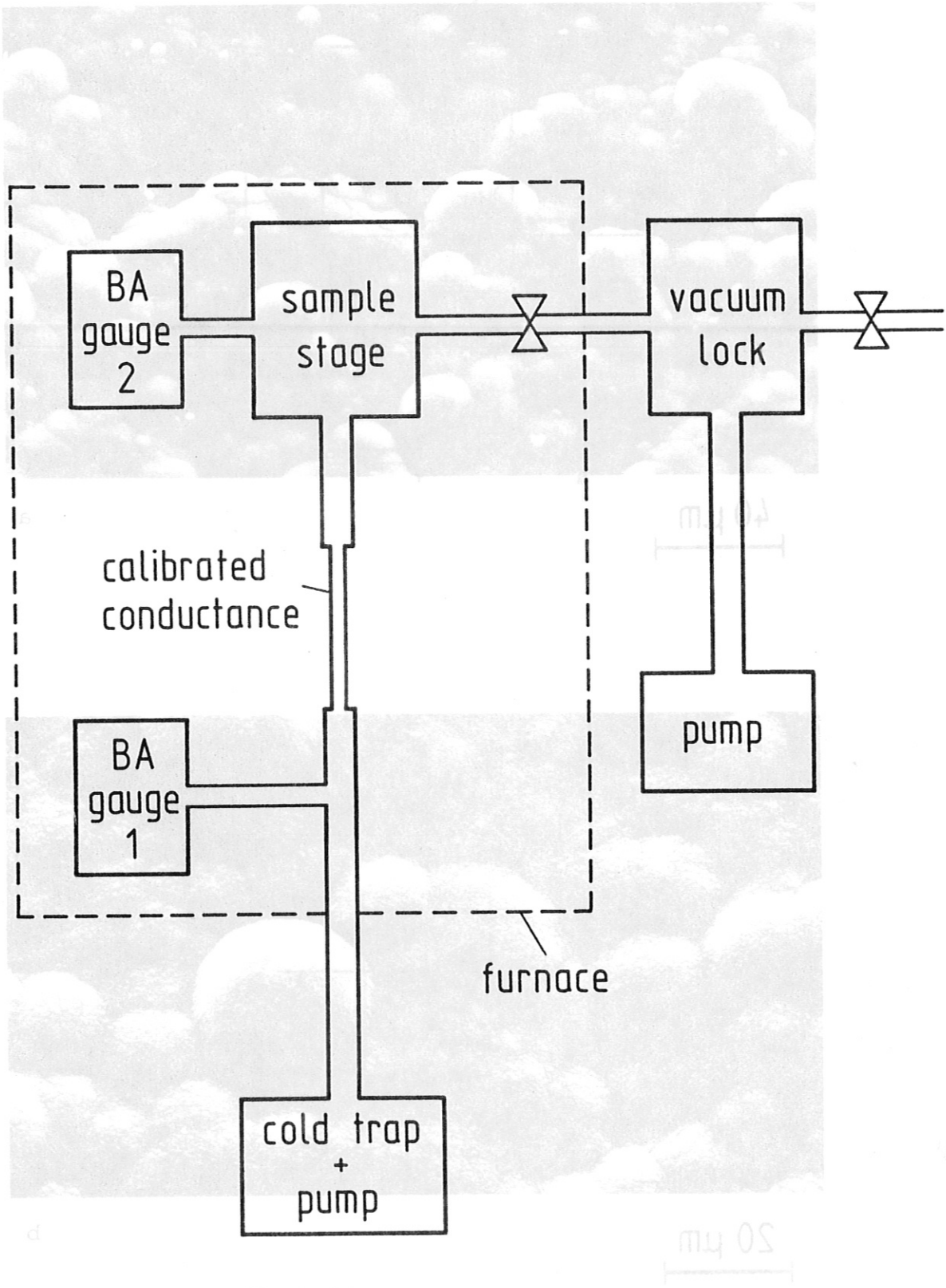


Fig. 3: Apparatus for measuring degassing rates.

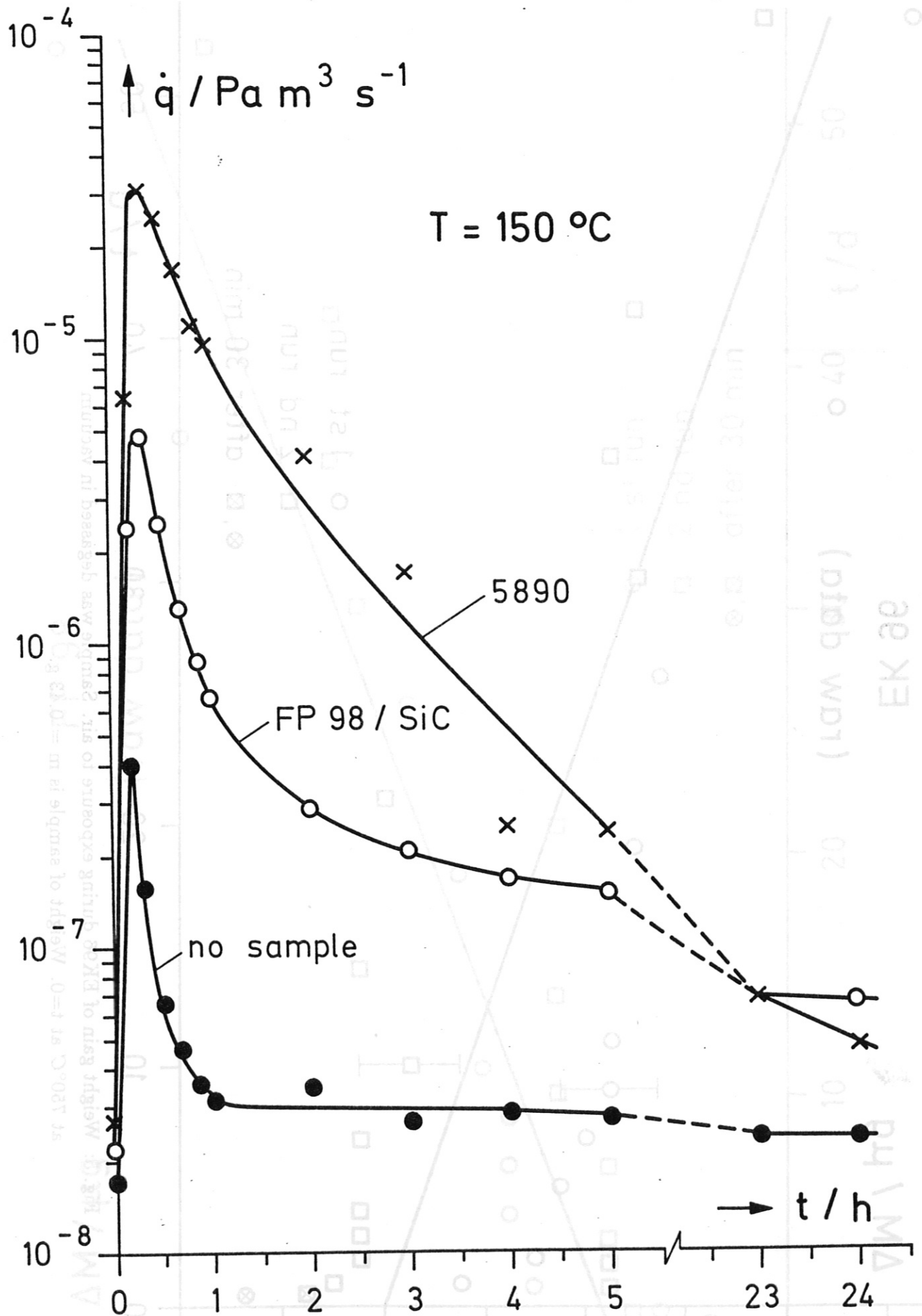


Fig. 4: Degassing rates of as-delivered samples at 150°C. $t = 0$ is the switching-on time of the furnace. The maximum degassing rate occurs shortly before 150°C is reached.

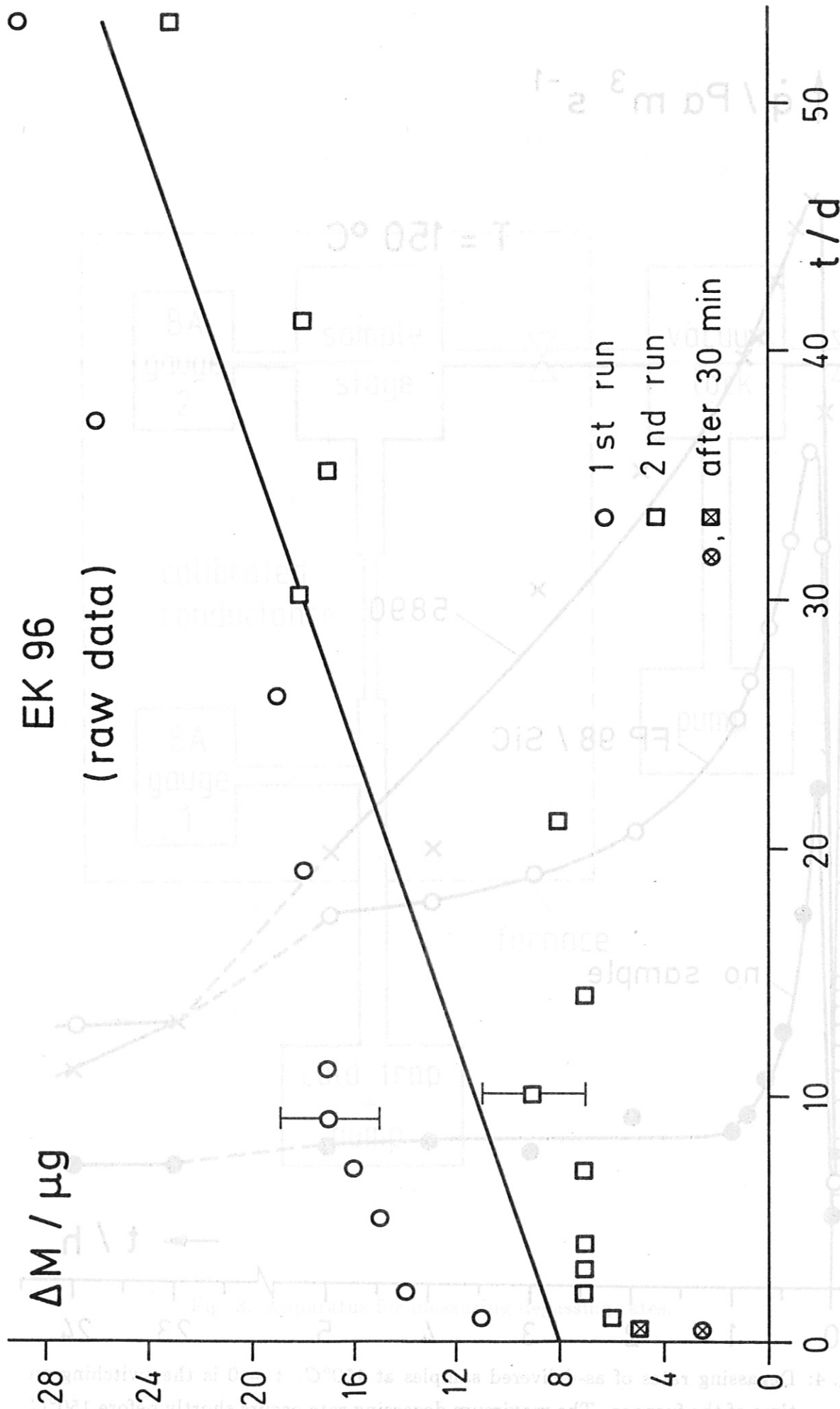


Fig. 5: Weight gain of EK96 during exposure to air. Sample was degassed in vacuum at 750°C at t=0. Weight of sample is m = 0.43 g.

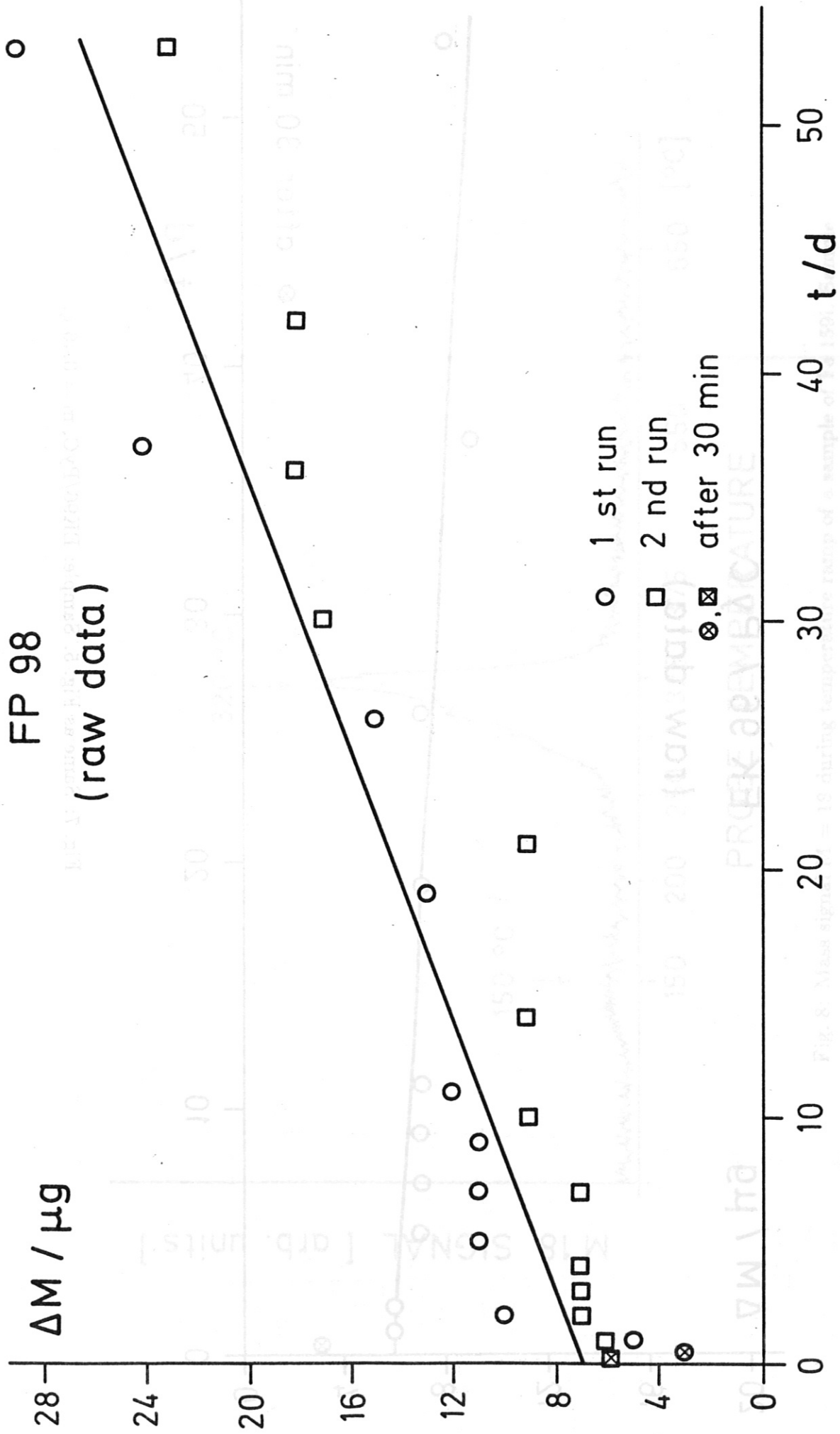


Fig. 6: Same as Fig. 5. Sample: FP98, $m = 0.36 \text{ g}$.

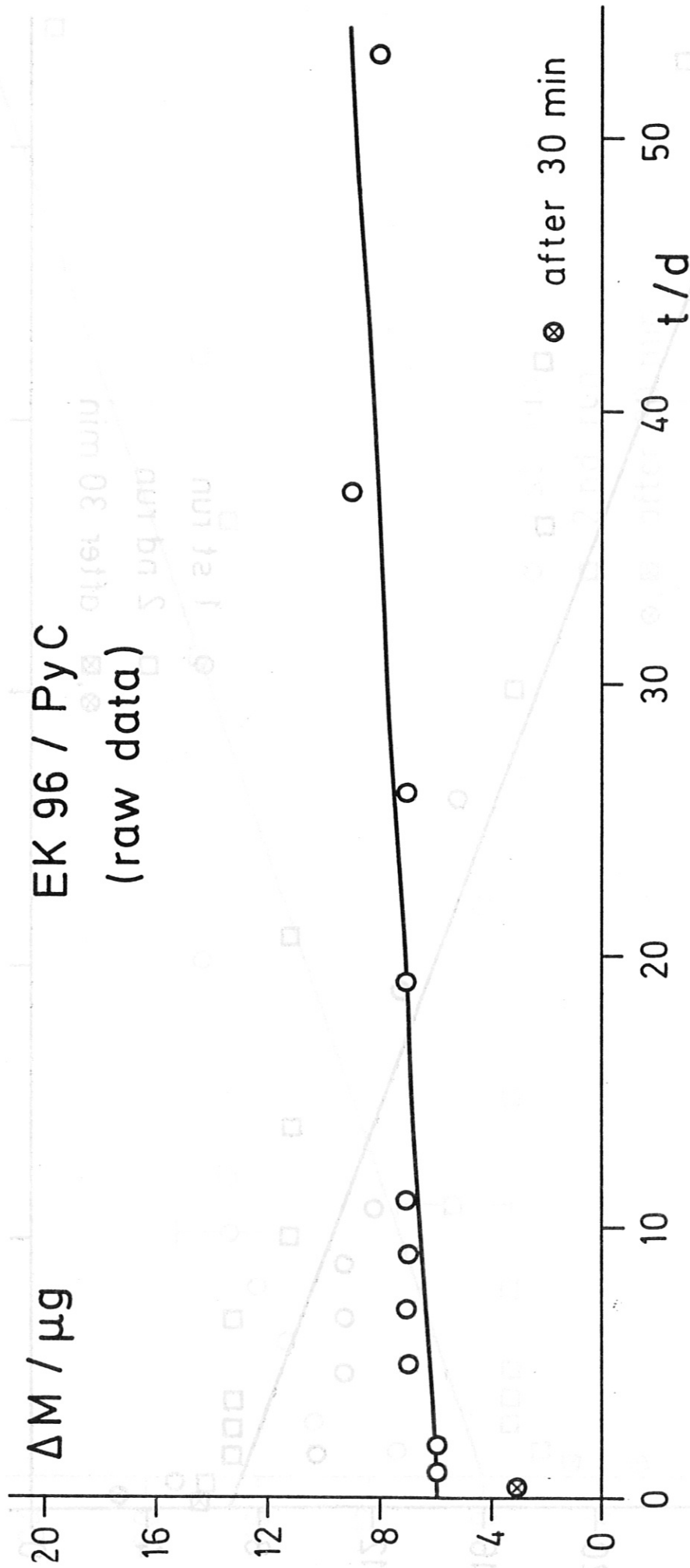


Fig. 7: Same as Fig. 5. Sample: EK96/PyC, m = 0.46 g.

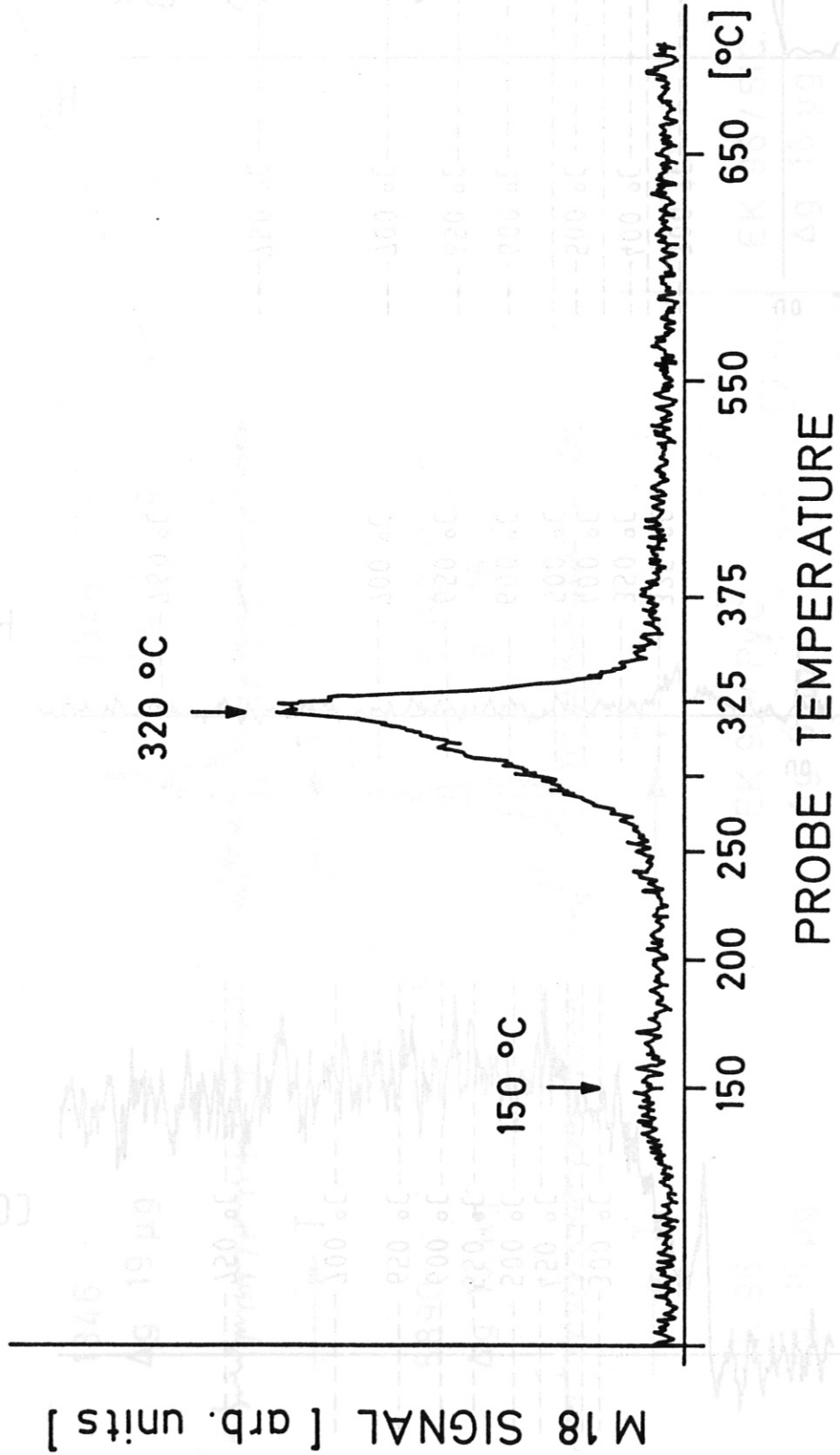


Fig. 8: Mass signal M = 18 during temperature ramp of a sample of Fe 159i. Sample was exposed to air for 1.5 days.

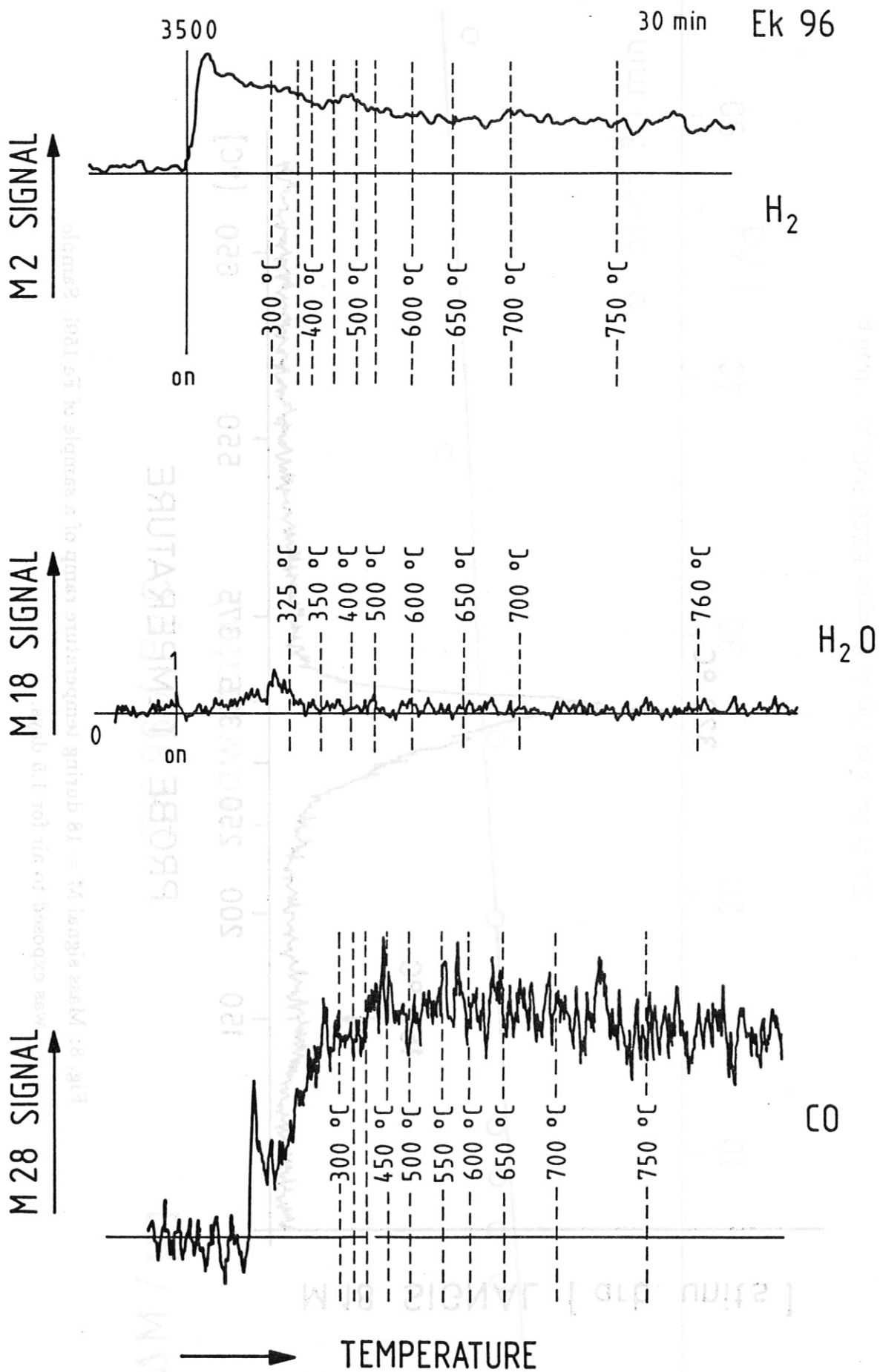


Fig. 9: Mass signal $M = 2$, $M = 18$ and $m = 28$ during temperature ramp of an EK96 sample.

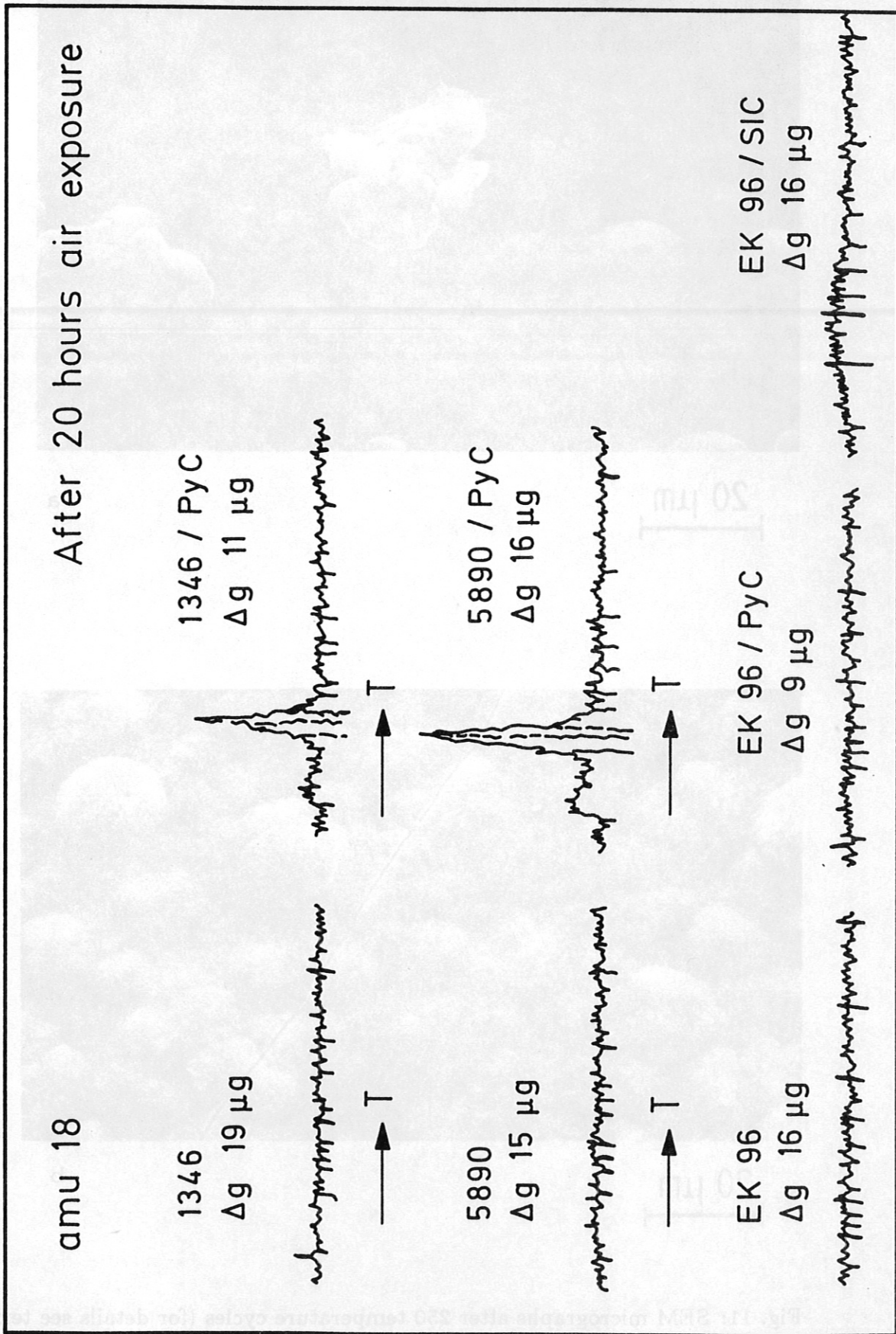
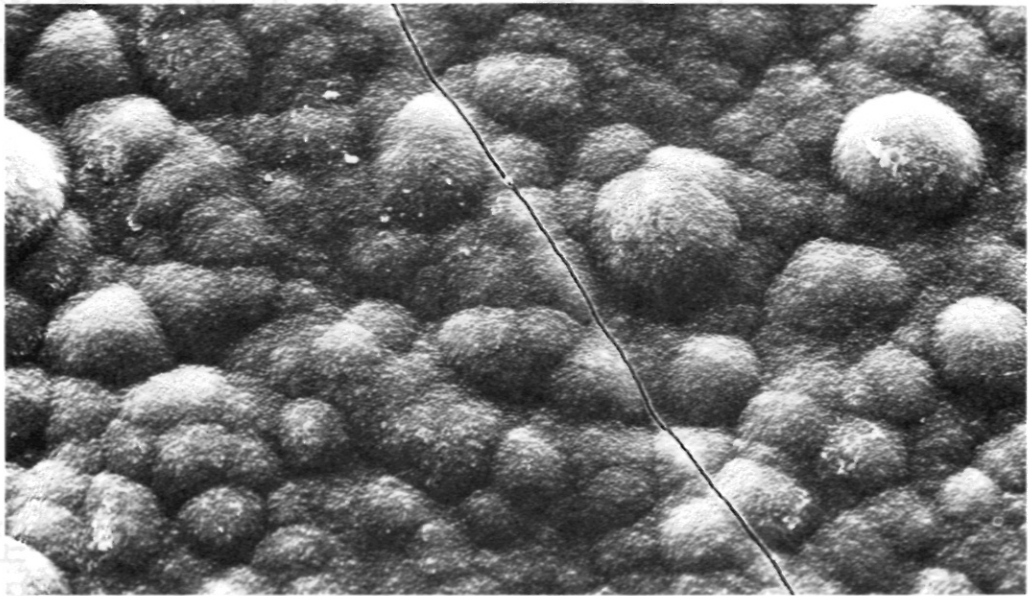


Fig. 10: Comparison of mass signals of M=18 for various samples. All samples exposed to air for 1 day.



20 μm

a



20 μm

b

Fig. 11: SEM micrographs after 250 temperature cycles (for details see text).

a) PyC coating; b) SiC coating.